Ordering and short-time orientational diffusion in dipolar hard-spherical colloids

O. Alarcón-Waess
Departamento de Física y Matemáticas, UDLA, Puebla, Santa Catarina Martir, Cholula 72820 Puebla, Mexico

E. Diaz-Herrera
Departamento de Física, UAM-I, Avenida Michoacan y Purisima, Colonía Vicentina, Iztapalapa, 09340 Mexico, Distrito Federal, Mexico

(Received 21 March 2001; revised manuscript received 3 October 2001; published 11 February 2002)

Orientational hydrodynamic functions and short-time, self-orientational and collective orientational diffusion coefficients of dipolar hard-spherical colloids are performed on a homogeneous isotropic phase, as functions of the wave vector q, for various values of the volume fraction and the dipolar strength of the macroparticles. The calculation is based on the dynamic orientational structure factor, which is the time-dependent self-correlation of the orientation density. We assume that the time evolution of the orientation density is given by the Smoluchoswki's equation, taking into account the hydrodynamic interactions as well as the dipolar interaction. The former are considered assuming pairwise additivity. The importance of the dynamic orientational structure factor is that its initial slope can be measured in a depolarized light scattering experiment. The results predict a different behavior for dilute and for dense dipolar colloids. The ordering phenomena are studied via the ordering coefficients, which are the orientational hydrodynamic functions at $q=0$. The results show that as the dipolar colloid evolves to the instability line, the translational ordering velocity increases while the rotational one reduces. The short-time orientational diffusion coefficients at $q=0$ are also performed. They predict that near to the instability line, the dipolar colloid diffuses translationally more than rotationally. At very dilute concentration the dipolar colloid presents an unexpected dynamical behavior, which seems to indicate that the colloid could be evolving to a reentrant phase.

DOI: 10.1103/PhysRevE.65.031402 PACS number(s): 82.70.Dd, 61.20.Gy, 61.20.Lc

I. INTRODUCTION

Collective relaxation of nonspherical colloids is not as well studied as that for spherical ones [1–4]. The importance of the collective relaxation is that it plays a key role in relaxation processes and also profoundly influences the dynamic behavior in the phase transitions [5]. The fundamental quantity to describe the collective relaxation is the dynamic structure factor $F(q,t)$, where q is the magnitude of the wave vector. Our purpose in this paper is to describe the collective translational rotational relaxation in dipolar hard-spherical colloids on a homogeneous isotropic phase. In order to carry out this study, we use the approach given by Alarcón-Waess, Diaz-Herrera, and Gil-Villegas in a recent paper [6] (hereafter referred to as I). This approach is based on the positional orientational behavior of the static orientational structure factor, which is the static self-correlation of the orientation density fluctuations.

In recent years the dipolar hard-spheres model has attracted much attention, since besides the fact that dipolar interactions are nearly omnipresent in molecular colloids, there are also several artificial systems where the dipolar interaction plays a dominant role [7]. The most important are the so-called ferrofluids, which are stable colloidal suspensions, i.e., colloidal iron particles, in a carrier liquid. A characteristic of the dipolar interaction is that it alone can break its symmetry and create a rich orientationally ordered colloidal suspension. At sufficiently low temperatures a dense system of dipolar hard spheres can spontaneously order into a ferroelectric state; however, for dilute systems the macroparticles are found to associate into chainlike structures with near contact of the hard spheres and head-to-tail alignment of the dipole moments [8–11]. Occasionally, at low concentration the colloid presents ring aggregates. In paper I, Alarcón-Waess, Diaz-Herrera, and Gil-Villegas predicted that for very dilute concentrations the dipolar colloid does not evolve into an orientationally ordered phase, as the dipolar strength is increased. Nevertheless the richness of the dipolar colloids, the effects of the collective translational rotational relaxation into the pretransitional dynamical behavior have not been studied much.

Up to now, the study of translational rotational dynamical behavior of the dipolar fluids has considered the fluctuations of the angular-dependent number density. Bagchi and Chandra have studied a dipolar liquid using an extended hydrodynamic description, where the slow variable is the angular-dependent number density [12]. They found that the orientational correlations slow down the collective orientational relaxation as compared to the single motion, which has important consequences in the pretransitional area near the isotropic-ordered liquid crystal transition. To compute the two-particle correlation function Bagchi and Chandra assumed that they are given by a linearized equilibrium theory. On the other hand, Hernández-Contreras *et al.* have computed the long-time self-diffusion coefficients, translational and rotational, as a function of the volume fraction and the dipolar strength of the macroparticles [13]. Their study is based on the generalized Langevin equation approach, neglecting the hydrodynamic interactions (HI). In this case, these authors consider as important variables the velocity of a dipolar macroparticle and the angular-dependent number density. To compute the equilibrium pair correlation distribution function, Hernández-Contreras *et al.* used the mean spherical approximation. The results obtained by these au-

thors show that the dipolar interaction leads to a strong suppression of both long-time self-diffusion coefficients, translational and rotational, compared with the corresponding free diffusion coefficient.

The main objective of this paper is to study the short-time dynamical behavior of a dipolar colloid as it evolves into the instability line [8]. Following the approach given in paper I, we will study the collective translational rotational relaxation of the orientation density into the short-time dynamical behavior of the dipolar hard-spherical colloids, on the homogeneous isotropic phase. As in paper I, the results are parametrized in terms of the refractive index of the scattering medium $n_s \sim k$. For simplicity, we parametrize the results by taking $k\sigma = 45/2$, where σ is the diameter of the colloidal particle.

In this paper, we focus our attention on the short-time self-diffusion and collective diffusion, and the orientational hydrodynamic functions, translational as well as rotational, of a dipolar colloid. In Sec. II, we develop a hydrodynamic description for the dipolar colloid. We use as a slow variable the orientation density. We assume that the dynamical behavior of the orientation density is given by Smoluchowski's equation, taking into account the HI and direct dipolar interactions. Following the definition of the self-correlation of the orientation density provided in paper I, we provide an expression for the dynamic orientational structure factor. The importance of this quantity is that its initial slope is related to the short-time collective orientational diffusion coefficients, whose expressions are provided as a function of $q\sigma$. We also provide expressions for the self-orientational diffusion coefficients and for the orientational hydrodynamic functions, translational as well as rotational, as functions of $q\sigma$. In Sec. III, we give our model system and the details for obtaining the angle-dependent pair correlation function using the reference hypernetted chain equation approach (RHNC). In Sec. IV, we compute the orientational hydrodynamic functions as a function of $q(\neq 0)$. Results for several values of the dimensionless dipolar strenght μ^{*2} and volume fraction ϕ are also provided. In Sec. V, we develop expressions for the short-time, collective orientational and self-orientational diffusion coefficients, translational and rotational, as functions of $q \neq 0$. We also provide results for several values of μ^{*2} and ϕ of the dipolar colloids. In Sec. VI, we compute the limit for very small wave vectors of the orientational hydrodynamic functions and for the short-time orientational diffusion coefficients. We interpretate the orientational hydrodynamic functions at $q=0$. The results for these quantities are reported as a function of μ^{*2} and ϕ of the dipolar colloids. Finally, in Sec. VII, the concluding remarks are given.

II. THEORETICAL APPROACH

According to paper I, we assume that the fundamental quantity to describe the collective translational rotational time-dependent behavior of dipolar colloids is the dynamic orientational structure factor $F(q,t)$. This quantity is the Fourier transform of the self-correlation of the local orientation density fluctuations occurring at different times, separated by the interval t. In particular, $F(q,t)$ is able to describe short-time behavior. This domain is defined for times t such that $\tau_B \ll t \ll \tau_I$, where τ_B is the Brownian relaxation time, which is the characteristic time for the relaxation of the translational velocity of a colloidal particle, and τ_I is the interaction time. τ_I is defined as the time for a macroparticle of translational diffusion coefficient D_T^0 to diffuse the distance $\sigma/2$. The importance of this approach is that the initial slope of $F(q,t)$ can be probed in a depolarized light scattering experiment, as a function of q, for very dilute concentrations [2].

Our starting point is the time-dependent self-correlation of the orientation density, $F(q,t)$ [Eq. (8) in paper I, evaluated at $t \neq 0$]. The orientation density is defined by [5]

$$\mathbf{Q}(q,t) = \frac{1}{\sqrt{N}} \sum_j \frac{3}{2}\left[\hat{\mathbf{u}}_j(t)\hat{\mathbf{u}}_j(t) - \frac{1}{3}\mathbf{I}\right] e^{i\mathbf{q}\cdot\mathbf{r}_j(t)}, \tag{1}$$

where $\hat{\mathbf{u}}_j(t)$ and $\mathbf{r}_j(t)$ are the unit vector in the direction of the dipole and the center of mass of the lth macroparticle, respectively. In order to describe the time evolution of $\mathbf{Q}(q,t)$, we assume that the dynamic of the colloid on time scales $t \gg \tau_B$ is entirely described in terms of a distribution function $P(\mathbf{r}^N, \Omega^N; t)$ [14], where $\mathbf{r}^N = (\mathbf{r}_1, \ldots, \mathbf{r}_N)$, $\Omega^N = (\Omega_1, \ldots, \Omega_N)$, and Ω_i denotes the polar angles that specify the direction of the ith dipole. The equation of motion of $P(\mathbf{r}^N, \Omega^N; t)$ is the generalized Smoluchowski equation [2],

$$\frac{\partial P(\mathbf{r}^N, \Omega^N; t)}{\partial t} = \mathbf{O}(\mathbf{r}^N, \Omega^N) P(\mathbf{r}^N, \Omega^N; t), \tag{2}$$

where $\mathbf{O}(\mathbf{r}^N, \Omega^N)$ is the Smoluchowski operator, and its adjoint is given by [15]

$$\tilde{\mathbf{O}}(\mathbf{r}^N, \Omega^N) = \sum_{ij} \left\{ \left[\frac{\partial}{\partial \mathbf{r}_i} - \beta\left(\frac{\partial \Phi}{\partial \mathbf{r}_i}\right)\right] \cdot \left[\mathbf{D}_{ij}^{TT} \cdot \frac{\partial}{\partial \mathbf{r}_j} + \mathbf{D}_{ij}^{TR} \cdot \mathbf{L}_j \right] + [\mathbf{L}_i - \beta(\mathbf{L}_i \Phi)] \cdot \left[\mathbf{D}_{ij}^{RR} \cdot \mathbf{L}_j + \mathbf{D}_{ij}^{RT} \cdot \frac{\partial}{\partial \mathbf{r}_j} \right] \right\}, \tag{3}$$

where $\mathbf{L}_i$ is the angular gradiant operator, $\Phi = \Phi(\mathbf{r}^N, \Omega^N)$ is the potential energy of the colloid, and $\mathbf{D}_{ij}^{ab} = \mathbf{D}_{ij}^{ab}(\mathbf{r}^N)$ are the microscopic diffusion tensors ($a,b = T,R$ means translational and rotational contributions, respectively). Assuming pairwise additivity of the HI, valid for small volume fractions [16], we have

$$\mathbf{D}_{11}^{aa} = D_a^0 \left[\mathbf{I} + \sum_j \{ A_s^a(r_{1j}) \hat{\mathbf{r}}_{1j} \hat{\mathbf{r}}_{1j} + B_s^a(r_{1j}) [\mathbf{I} - \hat{\mathbf{r}}_{1j} \hat{\mathbf{r}}_{1j}] \} \right] \tag{4}$$

and

$$\mathbf{D}_{ij}^{aa} = D_a^0 \{ A_c^a(r_{ij}) \hat{\mathbf{r}}_{ij} \hat{\mathbf{r}}_{ij} + B_c^a(r_{ij}) [\mathbf{I} - \hat{\mathbf{r}}_{ij} \hat{\mathbf{r}}_{ij}] \}, \tag{5}$$

where A_s^a, B_s^a and A_c^a, B_c^a are the self-mobility and cross-mobility functions, respectively. The solvent appears in Eq. (2) only through the (time-independent) diffusion tensors

$\mathbf{D}_{ij}^{ab}$. In Eqs. (4) and (5) D_a^0 are the translational ($a=T$) and rotational ($a=R$) diffusion coefficients, at infinite dilution.

Thus, the time development of the orientation density is given by

$$\mathbf{Q}(q,t)=e^{\tilde{\Omega}t}\mathbf{Q}(q,0). \tag{6}$$

In order to obtain a time-dependent expression for $F(q,t)$ in terms of the orientational diffusion coefficients, we start with the hydrodynamic description of the colloid. We choose as our hydrodynamic variables the orientation density and the translational and rotational fluxes [$\mathbf{J}_T(q,t)$ and $\mathbf{J}_R(q,t)$, respectively], which are related, in the simplest possible way, through the continuity equation

$$\frac{\partial \mathbf{Q}(q,t)}{\partial t}=-\boldsymbol{\nabla}_T\cdot\mathbf{J}_T(q,t)-\boldsymbol{\nabla}_R\cdot\mathbf{J}_R(q,t), \tag{7}$$

where $\boldsymbol{\nabla}_a$ represents the gradients in the Fourier and angular space, with $a=T,R$, respectively. The derivation of a model for the fluxes is based on the fact that in a dense colloid the relaxations of both spatial and angular orientational fluxes are very fast and only the orientation density is important on the time scale of interest [12]. At short times, the orientational fluxes are driven by their corresponding gradient in the orientation density of the colloid. For small gradients in the orientation density, the orientational fluxes are linear functions of these gradients, which can thus formally be written as

$$\mathbf{J}_a(q,t)=-\int dt' D_a(q,t-t')\boldsymbol{\nabla}_a\cdot\mathbf{Q}(q,t'), \tag{8}$$

where the integral kernel $D_a(q,t)$ will be referred to simply as the ''orientational diffusion coefficient,'' translational and rotational, which are functions of the orientation density. Using the nonlocal expression for the fluxes, Eq. (8), the Laplace transform of Eq. (7) and the definition of the dynamic orientational structure factor, we obtain

$$F(q,z)=[z+\Gamma_T(q)+\Gamma_R(q)]^{-1}F(q), \tag{9}$$

where $F(q)$ is the static orientational structure factor, which was performed in paper I, and the quantities $\Gamma_a(q)$ are the initial slope of $F(q,t)$,

$$\Gamma_a(q)=\nabla_a^2\frac{H_a(q)}{F(q)}. \tag{10}$$

We call the orientational hydrodynamic functions to the quantities, $H_a(q)$, which are essentially determined by the HI, via the microscopic diffusion tensors. It is also important to stress here that $H_a(q)$ are an ensamble average so that they also depend on the equilibrium distribution. The importance of the orientational hydrodynamic functions can be experimentally checked, since the initial slope and the static orientational structure factor can be probed in a depolarized light scattering experiment.

The orientational hydrodynamic functions versus $q\sigma$ are given by

$$H_a(q\sigma)=D_a^{s,short}(q\sigma)+H_a^d(q\sigma), \tag{11}$$

where $D_a^{s,short}(q\sigma)$ are the short-time self-orientational diffusion coefficients; the dimensionless translational one is given by

$$\frac{D_T^{s,short}(q\sigma)}{D_T^0}=1+\frac{\phi}{\sqrt{5\pi^3}}\int_1^\infty dx x^2 g(220;x)[3a_1(x)+a_2(x)]+\frac{\phi}{30}\sqrt{\frac{5}{14\pi^3}}\int_1^\infty dx x^2 g(222;x)a_2(x)S_T(q\sigma), \tag{12}$$

and the dimensionless rotational coefficient by

$$\frac{D_R^{s,short}}{D_R^0}=1+\frac{\phi}{\sqrt{5\pi^3}}\int_1^\infty dx x^2 g(220;x)[3b_1(x)+b_2(x)]+\frac{11\phi}{10}\sqrt{\frac{5}{14\pi^3}}\int_1^\infty dx x^2 g(222;x)b_2(x), \tag{13}$$

where $\phi=(\pi/6)\rho\sigma^3$, ρ is the bulk density, and the functions $a_l(x)$, $b_l(x)$, and $S_T(x)$, with $l=1$ and 2, are given in the Appendix. We must note that the short-time translational self-diffusion coefficient depends on n_s through the function $S_T(q\sigma)$ [see Eq. (9) in paper I], while the rotational coefficient is independent of n_s. The distinct parts of the orientational hydrodynamic functions are also provided; the dimensionless translational one is given by

$$\frac{H_T^d(q\sigma)}{D_T^0}=\frac{3}{8}\frac{\phi}{\sqrt{\pi^3}}\left\{3H_1^T(q\sigma)+4H_2^T(q\sigma)+\left[\frac{3}{2}H_3^T(q\sigma)+2H_4^T(q\sigma)\right]S_1(q\sigma)-[3H_5^T(q\sigma)+4H_6^T(q\sigma)]S_2(q\sigma)\right\}, \tag{14}$$

and the dimensionless rotational function by

$$\frac{H_R^d(q\sigma)}{D_R^0}=\frac{3}{2}\frac{\phi}{\sqrt{\pi^3}}\left\{H_1^R(q\sigma)+H_2^R(q\sigma)+\frac{1}{2}[H_3^R(q\sigma)+H_4^R(q\sigma)]S_1(q\sigma)+[H_5^R(q\sigma)+H_6^R(q\sigma)]S_2(q\sigma)\right\}, \tag{15}$$

where the functions $H_l^a(q\sigma)$ with $l=1,\ldots,6$, are given in terms of the projections of the angle-dependent pair correlation functions, as well as HI. As in the case of $F(q,0)$ the projections are only $g(22m;r)$ with $m=0$, 2, and 4. The functions $S_j(q\sigma)$, with $j=1,2$, $H_b^a(q\sigma)$, with $a=T,R$ and $b=1,\ldots,6$ are given in the Appendix.

The short-time collective orientational diffusion coefficients are given by

$$\frac{D_a^{c,short}(q\sigma)}{D_a^0} = \frac{D_a^{s,short}(q\sigma)}{D_a^0 F(q\sigma)} + \frac{H_a^d(q\sigma)}{D_a^0 F(q\sigma)}, \qquad (16)$$

where $a = T$ and R, correspond to the translational and rotational coefficients, respectively.

In summary, our results provide expressions, as functions of q, for the short-time self-orientational and collective orientational diffusion coefficients as well as for the orientational hydrodynamic functions. The advantage of these quantities is that they can be probed in a depolarized light scattering experiment. The next step is to compute the inputs $g(22l;r)$, since a linearized equilibrium theory is unable to calculate them; in the following section we provide and discuss the RHNC approach, which we use for obtaining these projections.

III. MODEL SYSTEM AND RHNC STRUCTURE

The model consists of hard spheres, in a carrier solution, with an embedded point dipole of strength μ at their center, where the dimensionless dipolar strength is defined as $\mu^{*2} = 1/T^*$, $T^* = k_B T\sigma^3/\mu^2$, and $k_B T$ is the thermal energy. The pair potential for molecules 1 and 2, with coordinates $(\mathbf{r}_1, \Omega_1)$ and $(\mathbf{r}_2, \Omega_2)$, is given by

$$u(1,2) = u_{HS}(r) + u_{DD}(\mathbf{r}, \Omega_1, \Omega_2), \qquad (17)$$

where $r = |\mathbf{r}| = |\mathbf{r}_2 - \mathbf{r}_1|$, $u_{HS}(r)$ is the usual hard-sphere potential and the dipolar potential is written as

$$u_{DD}(\mathbf{r}, \Omega_1, \Omega_2) = \frac{\mu^2}{r^3}[\hat{\mathbf{u}}_1 \cdot \hat{\mathbf{u}}_2 - 3(\hat{\mathbf{u}}_1 \cdot \hat{\mathbf{r}})(\hat{\mathbf{u}}_2 \cdot \hat{\mathbf{r}})]. \qquad (18)$$

For simplicity we use the notation $(1,2) \equiv (\mathbf{r}, \Omega_1, \Omega_2)$. The structural information of the dipolar colloid is contained in the total and direct correlation functions $h(1,2)$ and $c(1,2)$. On a homogeneous isotropic phase, these correlation functions are calculated by solving the Ornstein-Zernike equation

$$h(1,2) = c(1,2) + \frac{\rho}{4\pi}\int d3\, h(1,3)c(3,2), \qquad (19)$$

combined with the exact relation between $u(1,2)$, $h(1,2)$, $c(1,2)$, and the bridge function $B(1,2)$,

$$1 + h(1,2) = \exp[-\beta u(1,2) + h(1,2) - c(1,2) + B(1,2)]. \qquad (20)$$

In this work we use the RHNC approach [8,17], where $B(1,2)$ is approximated by the Verlet-Weiss expression of the underlying hard-sphere fluid. The solution of Eq. (19) is given in terms of projections of the angular-dependent pair correlation function $g(\mathbf{r}, \Omega_1, \Omega_2) = h(\mathbf{r}, \Omega_1, \Omega_2) + 1$, which are the coefficients of an expansion on a spherical invariant basis. Two different expansions are widely used depending on the choice of the reference frame [15]; we just use the laboratory one, which is given by

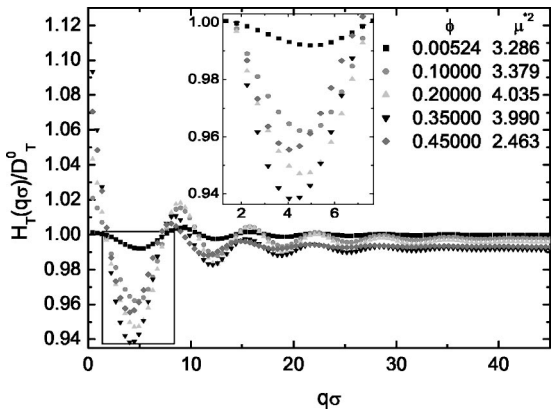

FIG. 1. Translational orientational hydrodynamic function as a function of $q\sigma$, for the values of ϕ and the corresponding highest values of μ^{*2} indicated in the figure.

$$g(\mathbf{r}, \Omega_1, \Omega_2) = \sum_{l_1 l_2 l} \sum_{m_1 m_2 m} g(l_1 l_2 l; r) C(l_1 l_2 l; m_1 m_2 m) \times Y_{l_1 m_1}(\Omega_1) Y_{l_2 m_2}(\Omega_2) Y_{lm}^*(\Omega_r), \qquad (21)$$

where $C(l_1 l_2 l; m_1 m_2 m)$ are the Clebsch-Gordan coefficients, $g(l_1 l_2 l; r)$ are the projections of the pair distribution functions, Ω_r represents the polar angles, which determines the direction of $\mathbf{r}$, and $Y_{lm}(\Omega)$ is the spherical harmonic.

IV. ORIENTATIONAL HYDRODYNAMIC FUNCTIONS

The orientational hydrodynamic functions contain the configuration-averaged effect of the HI on the short-time dynamics of the dipolar colloid. In case of vanishing HI, $H_a(q\sigma) = D_a^0$. To describe the complete behavior of the orientational hydrodynamic functions, we have investigated different regimes of ϕ at increasing μ^{*2}, as functions of the wave vector $(q \neq 0)$. We have defined five regimes and we have chosen a representative value of ϕ for each. The following increasing-dipole-strength regimes are considered: (1) the very low with $\phi = 0.005\,24$; (2) the low with $\phi = 0.1$ (chainlike regime); (3) the intermediate with $\phi = 0.2$ (mixed chainlike and ferroelectric regime); (4) the high with $\phi = 0.35$ (ferroelectric regime); and (5) the very high with $\phi = 0.45$ (ferroelectric regime). We have paid special attention to the very low regime, since it is the window in which the depolarized light scattering experiments can be performed, and in paper I an unexpected behavior was found.

In Fig. 1, we have plotted the translational orientational hydrodynamic function versus $q\sigma$ for each volume fraction and a value of the dipolar strength. The μ^{*2} chosen, for each ϕ, corresponds to the closest value to where the RHNC fail to have a solution. These values have already been obtained by Klapp and Fortsmann [8], except for the very low regime. They show that by increasing μ, from very high to low, the dipolar colloid reaches the instability line, which can be considered as the stability limit of the homogeneous isotropic phase. However, it is important to stress here that the RHNC predictions overestimate the temperatures when compared with the computer simulation values. From Fig. 1, we

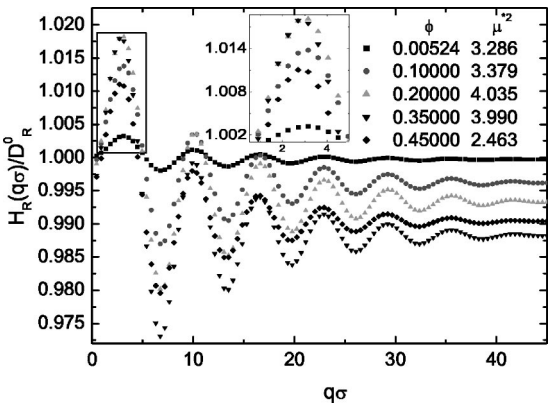

FIG. 2. Rotational orientational hydrodynamic function as a function of $q\sigma$, for the values of ϕ and the corresponding highest values of μ^{*2} indicated in the figure.

observe that the main peak is a minimum. In the inset, it can be seen that the depth of the minimum increases with ϕ until $\phi=0.35$, while for $\phi=0.45$ the depth does not increase, but decreases. In Fig. 2 we have plotted the rotational orientational hydrodynamic function versus $q\sigma$, for each ϕ and μ^{*2} of the regimes defined. Contrary to the translational function, here the main peak is a maximum. We observe that the height of the peak increases from the very low to the intermediate, while for high and very high regimes the peak decreases, as can be seen in the inset.

This different dynamical structural information requires a detailed study, which will not be given here. Nevertheless, we can say that this dynamical structural information could be related to the presence of different phases. Consequently, the orientational hydrodynamic functions present a different behavior for dilute and dense dipolar colloids, in agreement with previous results [6,8]. The precise value at which the dipolar colloid changes its behavior occurs for the translational function in $\phi=0.338$ and for the rotational one in $\phi=0.275$. These values were obtained at increments of $\Delta\phi=0.0125$. We have analyzed for other values of ϕ, but no different behavior was found. Comparing Figs. 1 and 2, we can observe that at very large q the translational function goes to 1 for all concentrations, while the rotational function goes to different values, depending on the concentration.

We can conclude that the HI produces a different behavior for dilute and dense dipolar colloids, in both orientational hydrodynamic functions. Nevertheless, we must note that the change in the translational and rotational behavior occurs at different concentrations. The translational response of the dipolar colloid requires a higher concentration to change its tendency than the rotational.

We focus our attention on the very low regime, since it is the window in which the experiments, using depolarized light scattering, can be performed; and according to paper I, in this regime the dipolar colloid exhibits an unexpected behavior. In order to analyze this regime, we have also plotted the orientational hydrodynamic functions for eight concentrations, from $\phi=0.002\,62$ to 0.0875. Unfortunately we could not observe any change, that is, the depth of the minimum and the height of the maximum always increase as ϕ is

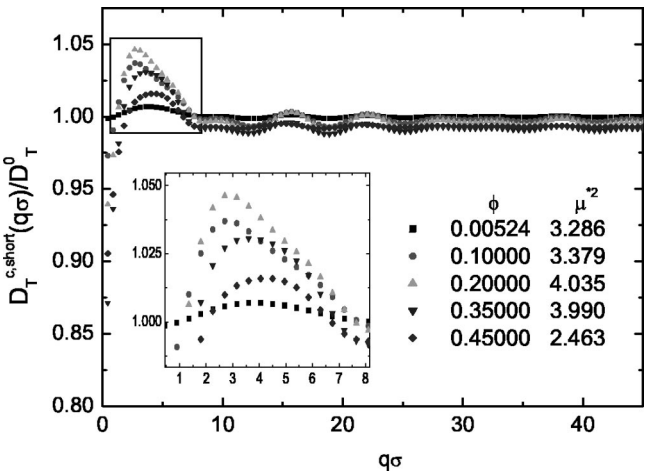

FIG. 3. Translational short-time collective orientational diffusion vs $q\sigma$ for different volume fractions and their corresponding highest value of dipolar strength, as indicated in the figure.

increased. We have considered it unnecessary to show them.

V. SHORT-TIME ORIENTATIONAL DIFFUSION

In this section, we describe the behavior of the short-time collective orientational and self-orientational diffusion coefficients as functions of $q\sigma\neq 0$. For the self-orientational case, we only consider the translational coefficient, since the rotational is independent of $q\sigma$. In order to analyze the short-time orientational diffusion coefficients, we have also considered the five regimes defined in the preceding section. In Fig. 3, we have plotted the translational short-time collective orientational diffusion coefficient, as function of $q\sigma$, for each ϕ and μ^{*2}. In this figure, we observe that for very large $q\sigma$ the coefficient goes to ~ 1. The height of the main maximum increases with ϕ until $\phi=0.2$ and then the peak decreases as ϕ is increased, as it can be seen in the inset. In the next plot, Fig. 4, we have now plotted the rotational short-time collective orientational diffusion coefficient, as a func-

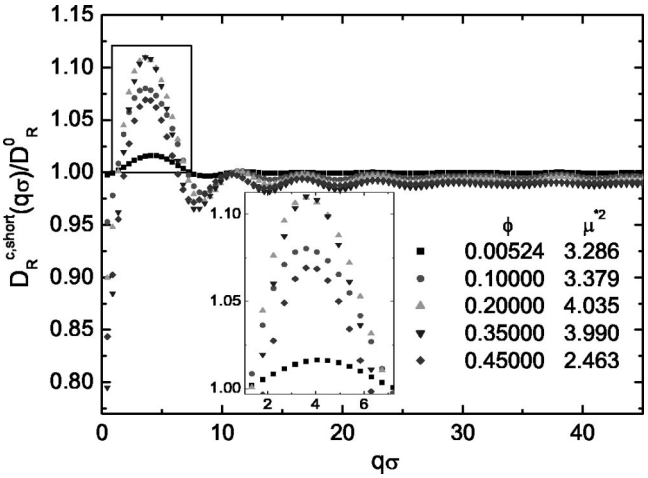

FIG. 4. Rotational short-time collective orientational diffusion versus $q\sigma$ for different volume fractions and their corresponding highest value of dipolar strength, as indicated in the figure.

tion of $q\sigma$, for each ϕ and μ^{*2}. This coefficient presents the same behavior of the translational coefficient. The main maximum also increases until $\phi=0.2$. The precise value in ϕ in which the peak increases is for the translational until $\phi=0.2125$ and for the rotational until $\phi=0.275$. As in the case of the orientational hydrodynamic functions, these values were found at increments of $\Delta\phi=0.0125$. From the results (Figs. 3 and 4), due to the HI, it is observed that the peak of the rotational coefficient is more enhanced than the translational.

We have also plotted the translational short-time self-orientational diffusion coefficient as a function of $q\sigma$. It is almost constant with $q\sigma$, the effect of HI is longer for dense dipolar colloids, and it is never longer than D_T^0. We have considered it unnecessary to show here.

The short-time orientational diffusion coefficients were also studied in the very low regime. But nothing is learned from them, so we have also considered it unnecessary to show them. From the results given in the preceding section and in this section, we can observe that the orientational hydrodynamic functions as well as the short-time orientational diffusion coefficients are very sensible at very small $q\sigma$. In the following section we focus our study on analyzing this observed feature.

VI. TRANSLATIONAL AND ROTATIONAL ORDER

According to paper I, the $q\sigma\rightarrow 0$ limit becomes the orientation density in the ordering tensor. Consequently, in this section the dynamical properties of a dipolar colloid are discussed taking only into account the orientations of the macroparticles. It is important to mention that the positional information of the macroparticles is also given through the angular-dependent pair correlation function. We focus our attention on the collective orientational behavior in the orientational hydrodynamic functions and the short-time orientational diffusion coefficients. To carry out this study, we have also considered the five regimes in ϕ defined in Sec. IV. We pay special attention to the very low regime, since it shows an unexpected behavior [6]. In the first subsection, we interpretate the $q\rightarrow 0$ limit of $H_a(q\sigma=0)$. We also describe the behavior of $H_a(q\sigma=0)$ as a function of ϕ and μ of the macroparticles. In the second subsection, the description of the short-time orientational diffusion coefficients at $q\sigma=0$ is given, as a function of ϕ and μ^{*2}.

A. Ordering coefficients

The generalized velocity of colloidal material is proportional to the total generalized force, that is,

$$\begin{pmatrix}\mathbf{v}_T(q,t)\\ \mathbf{v}_R(q,t)\end{pmatrix}=\begin{pmatrix}\mathbf{M}^{TT}[\mathbf{Q}(q,t)]\mathbf{M}^{TR}[\mathbf{Q}(q,t)]\\ \mathbf{M}^{RT}[\mathbf{Q}(q,t)]\mathbf{M}^{RR}[\mathbf{Q}(q,t)]\end{pmatrix}\times\begin{pmatrix}\boldsymbol{\nabla}_T \ln[\mathbf{Q}(q,t)]\dfrac{d\Pi[\mathbf{Q}(q,t)]}{d\mathbf{Q}(q,t)}\\ \boldsymbol{\nabla}_R\cdot\mathbf{Q}(q,t)\end{pmatrix}, \quad (22)$$

where $\mathbf{M}^{ab}[\mathbf{Q}(q,t)]$ are the mobility functions and $\Pi[\mathbf{Q}(q,t)]$ is the osmotic pressure [2]. Thus, in the $q\rightarrow 0$ limit the generalized velocities, translational and rotational, will be only given by the angular gradient of $\mathbf{Q}$. We define the ''ordering velocities'' as

$$\mathbf{v}_a(t)=\mathbf{M}^{aa}(q=0,t)\boldsymbol{\nabla}_R\cdot\mathbf{Q}(q=0,t). \quad (23)$$

Therefore, if we interpret as an external ordering field to the angular gradient of $\mathbf{Q}$, then ordering will be the phenomenon that dipolar colloidal particles attain certain ordering velocities, translational as well as rotational, under the action of this external ordering field. The ordering coefficients are the ratio of the ordering velocities, of a dipolar macroparticle in the colloid, to their values at infinity dilution. These coefficients evidently depend on ϕ and μ of the dipolar colloid, so that a measurement may be used for its characterization.

In order to calculate the ordering coefficients, we assume very weak inhomogeneities, i.e., the orientational fluxes are given by Fick's law, so Eq. (8) has the simplest form

$$\mathbf{J}_a(q,t)=-D_{\boldsymbol{\nabla}_a}\boldsymbol{\nabla}_a\cdot\mathbf{Q}(q,t), \quad (24)$$

where $D_{\boldsymbol{\nabla}_a}$ is the gradient orientational diffusion, which describes the transport of colloidal particles in an orientation density with a constant gradient. For very small wave vectors (large wavelengths), the short-time collective orientational diffusion coefficients are equal to the corresponding gradient orientational diffusion coefficients,

$$D_{\boldsymbol{\nabla}_a}=\lim_{q\rightarrow 0}D_a^{c,short}[\mathbf{Q}(q,t)]. \quad (25)$$

We consider a ''Gedanken experiment'' in which we assume a state in which the gradients in orientation density compensate for an ordering external field $\mathbf{E}_\mathbf{Q}$. To counterbalance the orientational diffusion fluxes, Eq. (24), with the corresponding fluxes driven by the ordering external field, given by

$$\mathbf{J}_{\mathbf{Q}_a}(q,t)=M^{aa}[\mathbf{Q}(q)]\mathbf{Q}(q,t)\mathbf{E}_{\mathbf{Q}_a}(q), \quad (26)$$

the ''ordering mobilities'' $M^{aa}[\mathbf{Q}(q)]$ must be proportional to the corresponding gradient orientational diffusion coefficients. As a consequence of this, the orientational hydrodynamic functions will be proportional to the corresponding ordering mobilities at $q=0$. Therefore, we obtain for the short-time regime the ordering velocities

$$\frac{v_{ord_a}}{v_{ord_a}^0}=\frac{H^{aa}(q\sigma=0)}{D_a^0}, \quad (27)$$

where $v_{ord_a}^0$ is the ordering velocity for an isolated particle in the same solvent.

From Eqs. (14) and (15) , the $q\rightarrow 0$ limit is, for the dimensionless translational ordering coefficient,

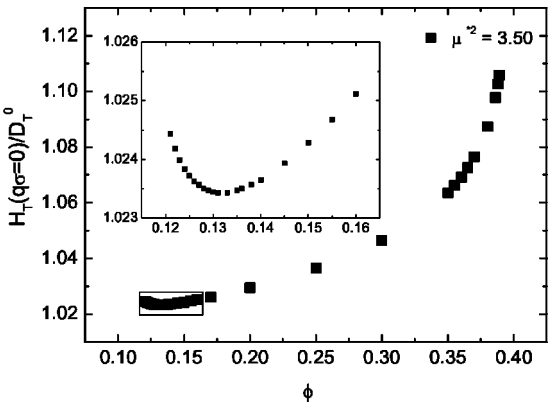

FIG. 5. Translational ordering coefficient as a function of ϕ for the isotherm indicated in the figure.

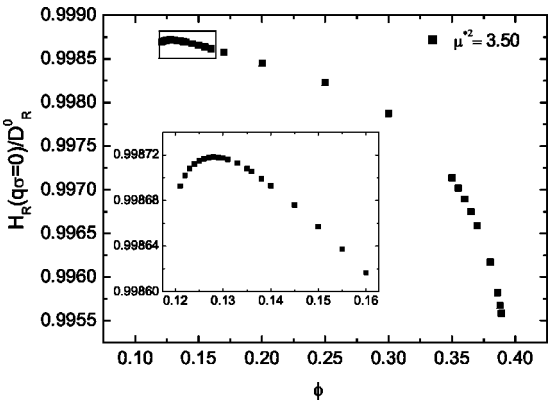

FIG. 6. Rotational ordering coefficient as a function of ϕ for the isotherm indicated in the figure.

$$\frac{H_T(q\sigma=0)}{D_T^0}=\frac{D_T^{s,short}(q\sigma=0)}{D_T^0}+\frac{\phi}{\sqrt{5\pi^2}}\left\{\frac{3}{2}\int_1^\infty dxxg(220;x)-\frac{3}{4}\frac{1}{\sqrt{14}}\int_1^\infty dxxg(222;x)+\int_1^\infty dxx^2[A_c^T(x)+2B_c^T(x)]g(220;x)-\frac{2}{\sqrt{14}}\int_1^\infty dxx^2[A_c^T(x)-B_c^T(x)]g(222;x)\right\}, \tag{28}$$

and for the dimensionless rotational coefficient,

$$\frac{H_R(q\sigma=0)}{D_R^0}=\frac{D_R^{s,short}}{D_R^0}+\frac{\phi}{\sqrt{5\pi^2}}\left\{6\int_1^\infty dxx^2[A_c^R(x)+2B_c^R(x)]g(220;x)-3\sqrt{\frac{2}{7}}\int_1^\infty dxx^2[A_c^R(x)-B_c^R(x)]g(222;x)\right\}, \tag{29}$$

where A_c^T, B_c^T, A_c^R, and B_c^R are the cross-mobility functions, which are given in the Appendix.

In Figs. 5 and 6, we show the ordering coefficients, as a function of ϕ, for the isotherm $T^*=0.286$ $[=(\mu^{*2}=3.5)^{-1}]$. Each value of ϕ, the highest and the lowest, corresponds to the closest point in which the RHNC fail to have a solution. We have chosen this isotherm since it has two points on the instability line [6,8], for the low and high value of ϕ. These figures show that, for intermediate values of ϕ, the ordering coefficients present a monotonic behavior as functions of the concentration. The translational coefficient increases while the rotational one decreases. That is, if the concentration is increased the translational ordering velocity becomes greater while the rotational one decreases, as a consequence of HI and of the dipolar interaction. From Figs. 5 and 6, we observe that when the dipolar colloid evolves into the instability line, it presents a different behavior for dilute and dense states. For the latter, the slope of the coefficients increases dramatically near of the instability line, while for dilute the slope reverses its sign and suffers a fast enlargement. The only difference, near the instability line, is that the translational coefficient enlarges while the rotational reduces. This behavior indicates that the translational ordering velocity enlarges, while the rotational one reduces, near the instability line.

The physical picture is, if the dipolar colloid evolves into the instability line, then the loss of rotational ordering velocity resulting from the tendency to align is offset by the gain in translational ordering velocity. It is important to mention that a similar behavior has been seen by Onsager in rods, he showed that as the concentration is increased, the rods; tend to align along a preferred direction, so in this nematic phase the loss of rotational entropy resulting from the aligment is offset by the gain in translational entropy [18]. In conclusion, we see that the behavior of the ordering coefficients, near the instability line, could be due to the presence of an orientationally ordered phase. This result is expected, because we are analyzing the response of a dipolar colloid to its orientational behavior, and this shows the tendency to lose its orientational symmetry. Thus, the ordering coefficients could be very important near an orientationally ordered phase.

In the next plots we show the ordering coefficients, as a function of μ^{*2}, for each ϕ of the regimes previously defined. For each plot, the maximun value of μ^{*2} corresponds to the closest point in which the RHNC fail to have a solution. In Fig. 7 we have plotted the translational ordering coefficient, while in the Fig. 8 that corresponding to the rotational ordering is plotted. In both figures, we observe that, for intermediate values of μ^{*2}, the ordering coefficients present the monotonic behavior discussed, which means that the dipolar colloid is far away from the instability line. While, for high values of μ^{*2}, we observe that from $\phi=0.45$ to 0.1, the ordering coefficients present the behavior previously discussed in Figs. 5 and 6. Consequently the dipolar colloid approaches the stability limit of the homogeneous isotropic phase [6,8]. For $\phi=0.1$, near the instability

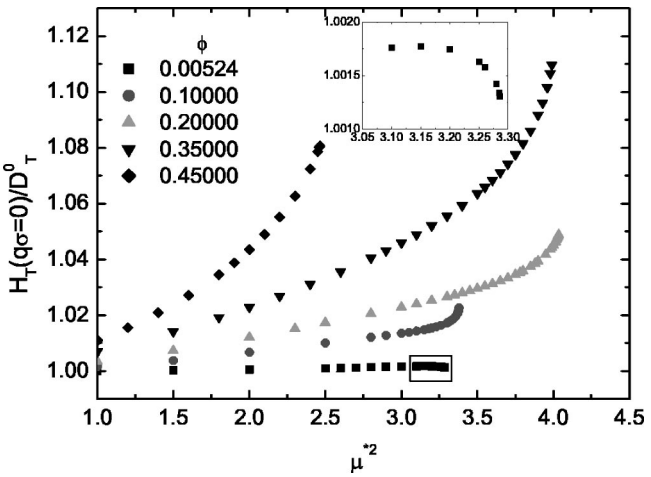

FIG. 7. Translational ordering coefficients as functions of μ^{*2} for the representative values in concentration for the five regimes.

line, we observe that the ordering coefficients enlarge suddenly their slope. This indicates that in the low regime the transition from the disordered to the ordered phase is obtainable in a progressive and continuous way, but near the instability line, a very rapid increment for the rotational is observed while for the translational a very rapid reduction is observed. A different behavior presents the very low regime ($\phi=0.005\,24$). The ordering coefficients first present the slope observed as if the dipolar colloid evolved the instability line, but near this line they suddenly invert and enlarge their slope. This unexpected behavior is in agreement with the results found for static properties in paper I. As can be seen in the inset of Figs. 5 and 6, the very low regime is characterized by a too small increment in its rotational ordering velocity, while the translational one presents a very small reduction.

We focus our attention on the very low regime, in order to analyze the characteristics observed. We have plotted, in Figs. 9 and 10, the ordering coefficients as a function of μ^{*2} for high values, from $\phi=0.002\,62$ to 0.0875 with increments of $\Delta\phi=0.0125$. The results show that there are three subregimes. In the first subregime for ϕ higher than 0.0524, the dipolar colloid evolves into the instability line. For the second subregime for concentrations between $\phi=0.0209$ and 0.0524, the dipolar colloid presents a suspicious behavior—the translational ordering resembles the behavior of an ordered phase, while the rotational ordering resembles a no ordered phase. In the third subregime for concentrations lower than $\phi=0.0209$, the dipolar colloid does not evolve into an orientationally ordered phase. The rotational ordering needs more concentration than the translational ordering to evolve into an orientationally ordered phase. For the third subregime, the ordering coefficients as a function of μ^{*2} first presents a slope as if the dipolar colloid evolved into the instability line, but near the transition, they suddenly invert and enlarge their slope. Thus, we see that the results predict that the phase reached in the third subregime may be a reentrant phase, which is characterized by a no global orientational order, in agreement with the prediction in paper I.

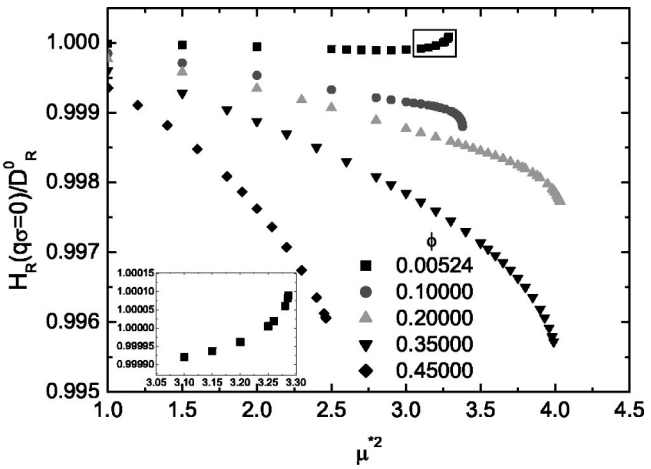

FIG. 8. Rotational ordering coefficients as functions of μ^{*2} for the representative values in concentration for the five regimes.

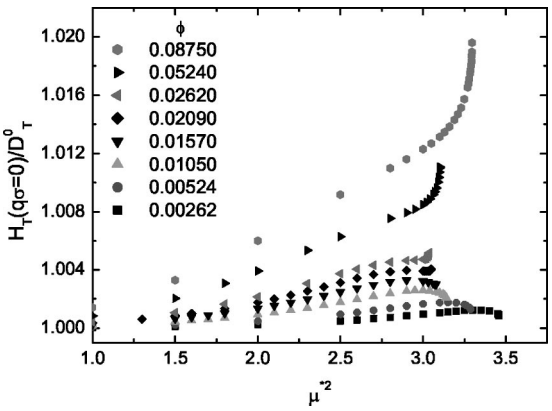

FIG. 9. Translational ordering coefficients as functions of μ^{*2} for the different concentrations as indicated in the figure.

B. Short-time orientational diffusion

In this subsection, we describe the short-time orientational diffusion of a dipolar colloid, taking into account only the ordering tensor fluctuations. From Eq. (16), in the very small wave vector limit, the short-time self-orientational and collective orientational diffusion coefficients can be obtained, as

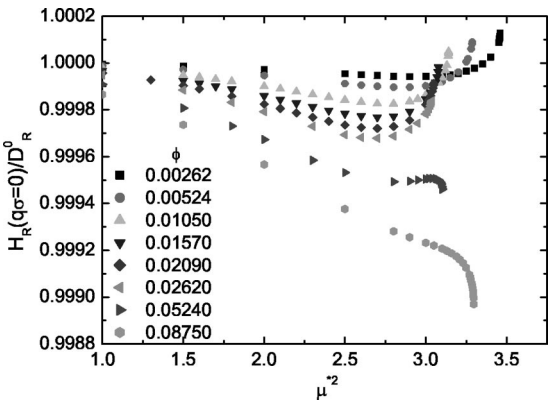

FIG. 10. Rotational ordering coefficients as functions of μ^{*2} for the different concentrations as indicated in the figure.

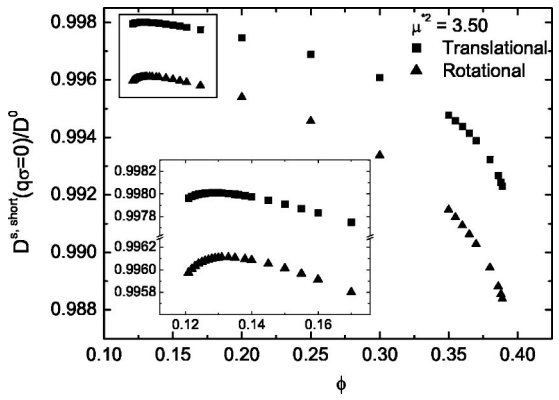

FIG. 11. Short-time self-orientational diffusion as a function of ϕ for the isotherm indicated in the figure at $q=0$. Translational and rotational.

functions of ϕ and μ^{*2}. As in the case of the ordering coefficients, we begin by analyzing the behavior of the colloid, via the short-time orientational diffusion, for when it evolves into the instability line. We again consider the isotherm $T^*=0.286[=(\mu^{*2}=3.5)^{-1}]$, which has two points on the instability line.

In Figs. 11 and 12, we have plotted the translational and rotational short-time, self-orientational and collective orientational diffusion coefficients respectively. From these figures, we can observe that, for intermediate values of ϕ, the four coefficients reduce monotonically as functions of ϕ. The HI effect is more pronounced for collective than for self-diffusion. In both short-time, self-orientational and collective orientational diffusion, the rotational is more suppressed than the translational. This behavior is already expected, since it is a consequence of the combined effects of the HI and the dipolar interaction. From Figs. 11 and 12, we can also observe that all the coefficients present a different behavior for dilute and dense concentrations near the instability line. For the latter, when the dipolar colloid evolves into the instability line, the slope of the coefficients enlarges very fast. For dilute, the situation, observed near the instability line, is that the slope inverts its sign and enlarges, as can be seen in the inset of each figure. Consequently, all the

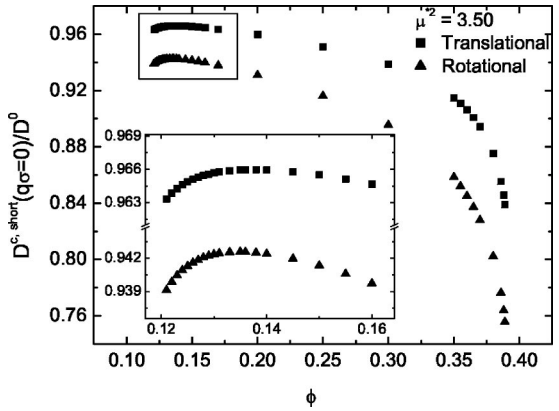

FIG. 12. Short-time collective orientational diffusion as function of ϕ for the isotherm indicated in the figure at $q=0$. Translational and rotational.

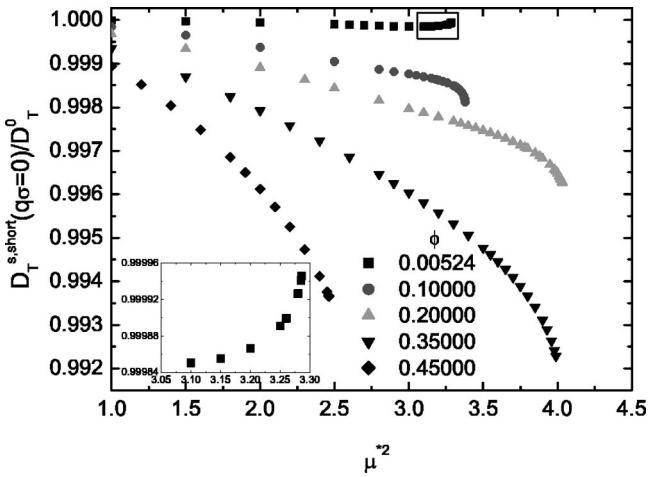

FIG. 13. Translational short-time self-orientational diffusion as a function of μ^{*2} for the representative values of each regime, as indicated in the figure at $q=0$.

coefficients reduce when the dipolar colloid approaches the instability line. In both figures (11 and 12), the rotational coefficients are more suppressed than the translational ones, specially near the instability line. Thus, near an orientationally ordered phase (instability line) a dipolar colloid is more restricted to diffuse rotationally than translationally.

Proceeding with the analysis, we study the short-time orientational diffusion coefficients in the five regimes defined in the Sec. IV. In Figs. 13–16, we have plotted the short-time orientational diffusion coefficients, as functions of μ^{*2}, for each regime. The maximun value of μ^{*2}, for each, is the closest point at which the RHNC fail to have a solution. As is indicated in each figure, they show the results for the translational and rotational short-time, self-orientational, and collective orientational diffusion coefficients. From very high to low, we find that for intermediate values of μ^{*2}, all the short-time orientational diffusion coefficients reduce monotonically as functions of ϕ. While, if the dipolar colloid approaches the instability line it enlarges its slope, as is expected, according to the behavior presented near the insta-

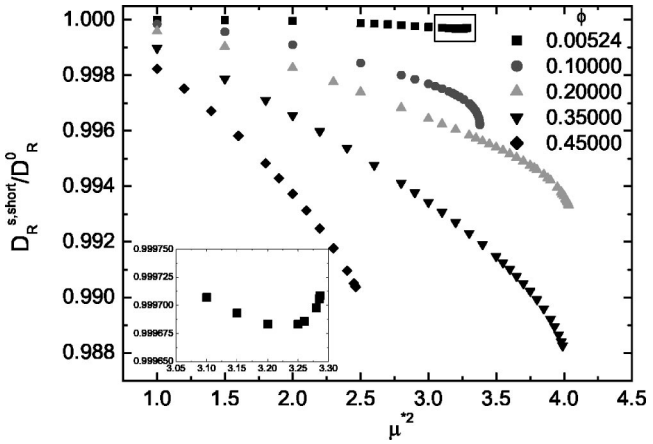

FIG. 14. Rotational short-time self-orientational diffusion as a function of μ^{*2} for the representative values of each regime, as indicated in the figure at $q=0$.

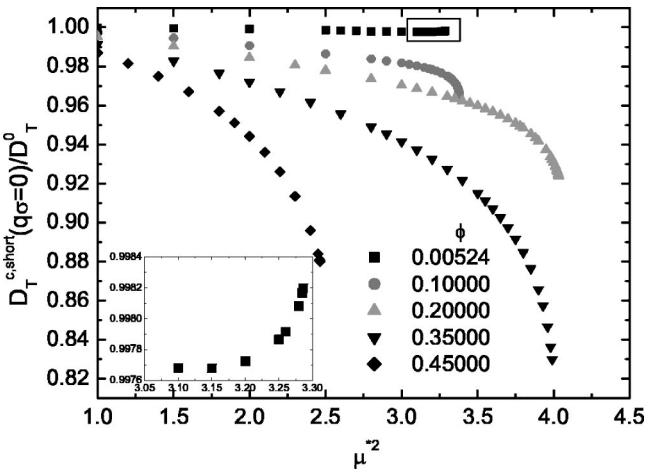

FIG. 15. Translational short-time collective orientational diffusion as a function of μ^{*2} for the representative values of each regime, as indicated in the figure at $q=0$.

bility line. For the low regime, the plots show that for all the coefficients its slope reduces, but near the instability line the reduction suddenly is larger; this behavior is also observed in the ordering coefficients. For the very low regime a different behavior is also observed in the Figs. 13–16. For each coefficient its slope is first reduced with μ^{*2}, but near the instability line it is invert and suffers a small enlargement. These results are in agreement with that found for the ordering coefficients and the results for static properties found in paper I.

We have analyzed for more concentrations in the very low regime from $\phi=0.002\,62$ to 0.0875. As is observed in Figs. 17–20, the results predict a similar behavior that described for the ordering coefficients. The precise values at which the coefficients will reach the instability line are: for the self-coefficient, translational until 0.005 24 and rotational until 0.0157, while for the collective, both until 0.0209. From the results for the self-coefficients, we can say that the dipolar colloid needs more concentration for the translational component than for the rotational one, for evolving into an ordered phase (instability line). However, from the collective coefficients, the concentration needed is the same for both components, translational and rotational.

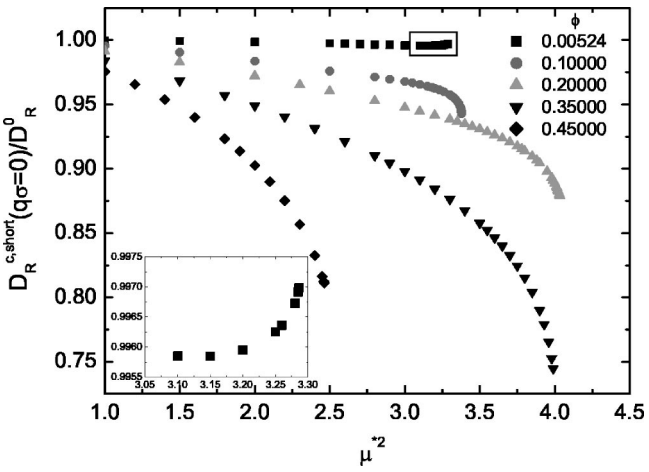

FIG. 16. Rotational short-time collective orientational diffusion as a function of μ^{*2} for the representative values of each regime, as indicated in the figure at $q=0$.

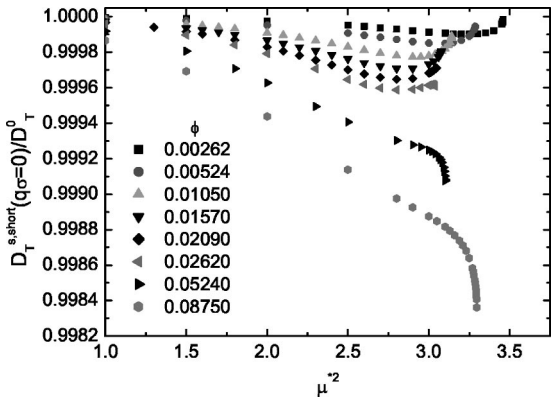

FIG. 17. Translational short-time self-orientational diffusion as a function of μ^{*2} for the values indicated in a the figure at $q=0$.

VII. CONCLUDING REMARKS

We have studied the short-time orientational diffusion and the ordering phenomenon of a dipolar hard-spherical colloid in an homogeneous isotropic phase. The study was based on the time-dependent fluctuational effects of the dynamic orientational structure factor, which is the self-correlation of the orientation density, for short times. The time evolution of the dynamic orientational structure factor is given by Smoluchowski's equation, taking into account the HI and dipolar interactions. The former was considered assuming pairwise additivity. All the quantities were studied as functions of the wave vector, for several values of the volume fraction and the dipolar strength. The results are parametrized by choosing the refractive index of the scattering medium, such that $k\sigma=45/2$. We have mainly focused our attention on the evolution of a dipolar colloid as a function of the dipolar strength, in order to predict its dynamical pretransitional behavior for different concentrations.

We have presented results for the translational and rotational short-time, self-orientational, and collective orienta-

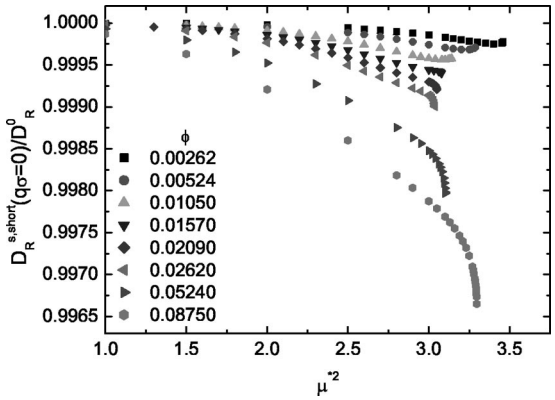

FIG. 18. Rotational short-time self-orientational diffusion as a function of μ^{*2} for the values indicated in the figure at $q=0$.

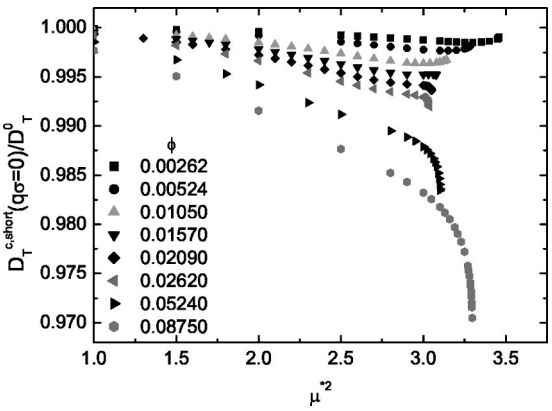

FIG. 19. Translational short-time collective orientational diffusion as a function of μ^{*2} for the values indicated in the figure at $q=0$.

tional diffusion coefficients, as a function of the wave vector. We have divided the analysis into five regimes, from very low to very high concentrations. All the coefficients were plotted as a function of the wave vector, for fixed values of ϕ and μ^{*2}. The latter was chosen as the closest point where the RHNC equations fail to have a solution. The results show that the dipolar colloid has a different behavior for dilute and dense concentrations. For the same regimes, we have also studied the orientational hydrodynamic functions, as a function of the wave vector. The results also show that the dipolar colloid presents a different behavior for dilute and dense concentrations.

The study of the ordering phenomenon has been performed via the ordering coefficients, which are proportional to the ordering velocities, and the coefficients are the orientational hydrodynamic functions at $q=0$. These ordering velocities cause the dipolar colloid to lose some positional and/or orientational symmetries. Our results show that if a dipolar colloid evolves into the instability line, the translational ordering coefficient increases while the rotational one reduces. The physical picture is that the loss of rotational ordering velocity resulting from the tendency to align is offset by the gain in translational ordering velocity. Consequently, near the instability line, the rotational ordering coefficient decreases due to the loss of orientational symmetry, while the translational coefficient increases, compensating the loss.

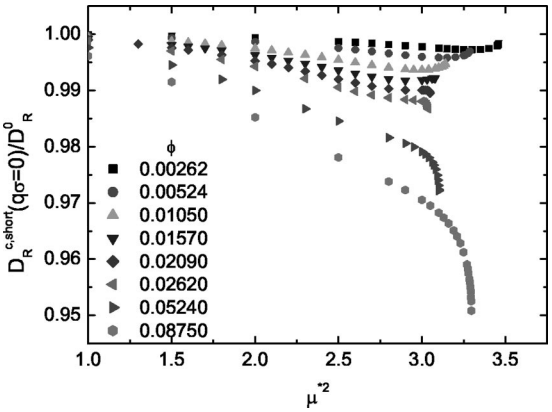

FIG. 20. Rotational short-time collective orientational diffusion as a function of μ^{*2} for the values indicated in the figure at $q=0$.

Related to the short-time self-orientational and collective-orientational diffusion coefficients at $q=0$, translational as well as rotational, coefficients reduce when a dipolar colloid approaches the instability line. The HI effect is more pronounced for collective than for self-orientational diffusion. Concerning the translational and rotational coefficients, the latter is more suppressed than the former. Consequently, near the instability line, the dipolar colloid is more restricted to being diffuse rotationally than translationally, due to the alignment.

Our results predict the dynamical behavior at short times, near the instability line, from very high to low concentrations. In the low regime, the approximation to the instability line is obtained in a progressive way, but near the line suddenly the dipolar colloid tends to align quickly. Our main prediction is that in the very low regime the dipolar colloid may have a reentrant phase. For concentrations lower than $\phi=0.0209$, the dipolar colloid behaves as if it will evolve into the instability line, but near the transition it changes its behavior, coming back to a phase with no global orientational order. These results are in agreement with the predictions for the static case, presented in paper I. The relevance of the results performed for the very low regime case is that they can be measured in a depolarized light scattering experiment. A direct comparison with experiments is anticipated in order to test the validity of the conclusions given in this paper.

ACKNOWLEDGMENT

This work was supported by funds from CONACYT, Mexico, Grant No. 28239 E.

APPENDIX

We give the functions that appear in Eqs. (12) and (13):

$$a_1(x)=-\frac{17}{1024}\frac{1}{x^6}-\frac{5}{1024}\frac{1}{x^8}+\frac{141}{16384}\frac{1}{x^{10}}+O(x^{-12}), \tag{A1}$$

$$a_2(x)=-\frac{15}{64}\frac{1}{x^4}-\frac{105}{1024}\frac{1}{x^6}+\frac{373}{8192}\frac{1}{x^8}-\frac{1385}{16384}\frac{1}{x^{10}}+O(x^{-12}), \tag{A2}$$

$$S_T(x)=1+3\left[1-2\left(\frac{x}{30}\right)^2\right]^3, \tag{A3}$$

$$b_1(x)=-\left[\frac{15}{256}\frac{1}{x^6}+\frac{39}{1024}\frac{1}{x^8}+\frac{18}{1024}\frac{1}{x^{10}}+\frac{835}{65536}\frac{1}{x^{12}}+O(x^{-14})\right], \tag{A4}$$

$$b_2(x)=\frac{15}{256}\frac{1}{x^6}+\frac{27}{1024}\frac{1}{x^8}+\frac{12}{1024}\frac{1}{x^{10}}+\frac{675}{65536}\frac{1}{x^{12}}+O(x^{-12}). \tag{A5}$$

We give the functions that appear in Eqs. (14) and (15):

$$H_1^T(y)=-\frac{1}{2}\int_1^\infty dx x\left[-\frac{1}{\sqrt{5}}g(220;x)FG_{00}(yx)+\frac{1}{\sqrt{14}}g(222;x)FG_{20}(yx)+\sqrt{\frac{8}{35}}g(224;x)FG_{40}(yx)\right], \tag{A6}$$

$$H_2^T(y)=-\int_1^\infty dx x^2\left\{-\frac{1}{\sqrt{5}}g(220;x)\{B_c'(x)F_{00}(yx)+[A_c'(x)-B_c'(x)]G_{00}(yx)\}+\frac{1}{14}g(222;x)\times\{B_c'(x)F_{20}(yx)+[A_c'(x)-B_c'(x)]G_{20}(yx)\}+\sqrt{\frac{8}{35}}g(224;x)\{B_c'(x)F_{40}(yx)+[A_c'(x)-B_c'(x)]G_{40}(yx)\}\right\}, \tag{A7}$$

$$H_3^T(y)=-\frac{1}{2}\int_1^\infty dx x\left[-\sqrt{\frac{3}{7}}g(222;x)FG_{22}(yx)+\frac{1}{\sqrt{7}}g(224;x)FG_{42}(yx)\right], \tag{A8}$$

$$H_4^T(y)=-\int_1^\infty dx x^2\left\{-\frac{3}{\sqrt{7}}g(222;x)\{B_c'(x)FF_{22}(yx)+[A_c'(x)-B_c'(x)]GG_{22}(yx)\}+\frac{2}{\sqrt{7}}g(224;x)\times\{B_c'(x)FF_{42}(yx)+[A_c'(x)-B_c'(x)]GG_{42}(yx)\}\right\}, \tag{A9}$$

$$H_5^T(y)=-\frac{1}{2}\int_1^\infty dx x\left[-\sqrt{\frac{3}{7}}g(222;x)FG_{\underline{22}}(yx)+\frac{2}{\sqrt{7}}g(224;x)FG_{\underline{42}}(yx)\right], \tag{A10}$$

$$H_6^T(y)=-\int_1^\infty dx x^2\left\{-\frac{3}{\sqrt{7}}g(222;x)\{B_c'(x)FF_{\underline{22}}(yx)+[A_c'(x)-B_c'(x)]GG_{\underline{22}}(yx)\}+\frac{2}{\sqrt{7}}g(224;x)\times\{B_c'(x)FF_{\underline{42}}(yx)+[A_c'(x)-B_c'(x)]GG_{\underline{42}}(yx)\}\right\}, \tag{A11}$$

$$A_c'(x)=-\frac{1}{8}\frac{1}{x^3}+\frac{75}{512}\frac{1}{x^7}+O(x^{-9}), \tag{A12}$$

$$B_c'(x)=\frac{1}{16}\frac{1}{x^3}+O(x^{-11}), \tag{A13}$$

$$H_1^R(y)=\int_1^\infty dx x^2 B_c^R(x)\left[\frac{6}{\sqrt{5}}g(220;x)F_{00}^R(yx)-\frac{3}{2}\sqrt{\frac{2}{7}}g(222;x)F_{20}^R(yx)+8\sqrt{\frac{2}{35}}g(224;x)F_{40}^R(yx)\right], \tag{A14}$$

$$H_2^R(y)=\int_1^\infty dx x^2[A_c^R(x)-B_c^R(x)]\left\{g(220;x)\left[\frac{5}{2\sqrt{5}}H_{00}^R(yx)+\frac{1}{\sqrt{5}}G_{00}^R(yx)\right]+g(222;x)\left[-\frac{1}{2}\sqrt{\frac{2}{7}}H_{00}^R(yx)-\frac{1}{\sqrt{14}}G_{20}^R(yx)+\sqrt{\frac{3}{7}}FF_{22}^R(yx)+\frac{3}{2}\sqrt{\frac{3}{7}}GG_{\underline{21}}^R(yx)\right]+g(224;x)\left[5\sqrt{\frac{2}{35}}H_{40}^R(yx)-2\sqrt{\frac{2}{35}}G_{40}^R(yx)+\frac{3}{2\sqrt{7}}FF_{42}^R(yx)-\sqrt{\frac{2}{7}}GG_{\underline{41}}^R(yx)\right]\right\}, \tag{A15}$$

$$H_3^R(y)=\int_1^\infty dx x^2 B_c^R(x)\left[3\sqrt{\frac{3}{7}}g(222;x)GG_{22}^R(yx)+\frac{8}{\sqrt{7}}g(224;x)GG_{42}^R(yx)\right], \tag{A16}$$

$$H_4^R(y)=\int_1^\infty dx x^2[A_c^R(x)-B_c^R(x)]\Bigg\{ g(222;x)\times\Bigg[-3\sqrt{\frac{2}{7}}K_{20}^R(yx)+2\sqrt{\frac{3}{7}}KK_{22}^R(yx)-\sqrt{\frac{3}{7}}LL_{22}^R(yx)+3\sqrt{\frac{3}{7}}LL_{\underline{21}}^R(yx)\Bigg]+g(224;x)\times\Bigg[9\sqrt{\frac{2}{35}}K_{40}^R(yx)+GG_{44}^R(yx)+\frac{3}{\sqrt{7}}KK_{42}^R(yx)+\sqrt{\frac{2}{7}}LL_{42}^R(yx)+3\sqrt{\frac{2}{7}}LL_{\underline{41}}^R(yx)+\frac{2}{\sqrt{2}}LL_{\underline{43}}^R(yx)\Bigg]\Bigg\}, \tag{A17}$$

$$H_5^R(y)=-\int_1^\infty dx x^2 B_c^R(x)\Bigg[3\sqrt{\frac{3}{7}}g(222;x)GG_{\underline{22}}^R(yx)+\frac{8}{\sqrt{7}}g(224;x)GG_{\underline{42}}^R(yx)\Bigg], \tag{A18}$$

$$H_6^R(y)=-\int_1^\infty dx x^2[A_c^R(x)-B_c^R(x)]\Bigg\{ g(222;x)\times\Bigg[2\sqrt{\frac{3}{7}}KK_{\underline{22}}^R(yx)-\sqrt{\frac{3}{7}}LL_{\underline{22}}^R(yx)-\sqrt{\frac{3}{7}}LL_{\underline{21}}^R(yx)\Bigg]+g(224;x)\Bigg[GG_{\underline{44}}^R(yx)+\frac{3}{\sqrt{7}}KK_{\underline{42}}^R(yx)+\sqrt{\frac{2}{7}}LL_{\underline{42}}^R(yx)+3\sqrt{\frac{2}{7}}LL_{41}^R(yx)+\frac{2}{\sqrt{2}}LL_{43}^R(yx)\Bigg]\Bigg\}, \tag{A19}$$

$$A_c^R(x)=\frac{1}{8}\frac{1}{x^3}+O(x^{-13}), \tag{A20}$$

$$B_c^R(x)=-\frac{1}{16}\frac{1}{x^3}+O(x^{-9}). \tag{A21}$$

We do not give the explicit expressions for the undefined functions in the last equations, those that appear in the orientational hydrodynamic functions, because nothing is learned from them. They are provided from the authors by request.

[1] G. Naegele, Phys. Rep. **272**, 215 (1996).
[2] J. K. G. Dhont, *An Introduction to Dynamics of Colloids* (Elsevier, New York, 1996).
[3] M. Hernández-Contreras and M. Medina-Noyola, Phys. Rev. E **54**, 6573 (1996).
[4] M. Hernández-Contreras, M. Medina-Noyola, and O. Alarcón-Waess, Physica A **231**, 62 (1996).
[5] M. P. Allen, G. T. Evans, D. Frenkel, and B. M. Mulder, in *Advances in Chemical Physics*, edited by I. Prigogine and S. A. Rice (Wiley, New York, 1993), Vol. LXXXVI.
[6] O. Alarcón-Waess, E. Diaz-Herrera, and A. Gil-Villegas Phys. Rev. E (to be published).
[7] R. E. Rosensweig, Sci. Am. **247**, 124 (1982); *Ferrodynamics* (Cambridge University, New York, 1985).
[8] S. Klapp and F. Fortsmann, J. Chem. Phys. **106**, 9742 (1997).
[9] D. Levesque and J. J. Weis, Phys. Rev. E **49**, 5131 (1994).
[10] D. Wei and G. N. Patey, Phys. Rev. Lett. **68**, 2043 (1992).
[11] J. J. Weis and D. Levesque, Phys. Rev. E **48**, 3728 (1993).
[12] B. Bagchi and A. Chandra, in *Advances in Chemical Physics*, edited by I. Prigogine and S. A. Rice (Wiley, New York, 1991), Vol. LXXX.
[13] M. Hernández-Contreras, P. González-Mozuelos, O. Alarcón-Waess, and H. Ruíz-Estrada, Phys. Rev. E **57**, 1817 (1998).
[14] C. Gray and K. E. Gubbins, *Theory of Molecular Fluids* (Clarendon Press, Oxford, 1984).
[15] R. B. Jones and P. N. Pusey, Annu. Rev. Phys. Chem. **42**, 137 (1991).
[16] R. Schmitz and B. U. Felderhof, Physica A **116**, 163 (1982).
[17] M. Kasch and F. Forstmann, J. Chem. Phys. **99**, 3037 (1993).
[18] L. Onsager, Phys. Rev. **62**, 558 (1942); Ann. N.Y. Acad. Sci. **51**, 627 (1949).